

Fundamentals of PV efficiency interpreted by a two-level model

Muhammad A. Alam and M. Ryyan Khan

Citation: *American Journal of Physics* **81**, 655 (2013); doi: 10.1119/1.4812594

View online: <http://dx.doi.org/10.1119/1.4812594>

View Table of Contents: <http://scitation.aip.org/content/aapt/journal/ajp/81/9?ver=pdfcov>

Published by the [American Association of Physics Teachers](#)

Articles you may be interested in

[Enhancing student learning of two-level quantum systems with interactive simulations](#)

Am. J. Phys. **83**, 560 (2015); 10.1119/1.4913786

[Cavity quantum electrodynamics of a two-level atom with modulated fields](#)

Am. J. Phys. **80**, 612 (2012); 10.1119/1.3703016

[The Statistical Interpretation of Entropy: An Activity](#)

Phys. Teach. **48**, 516 (2010); 10.1119/1.3502501

[On the problem of observation of two-level tunneling states in supercooled liquids, glass-forming polymers, orientational glasses, and metallic glasses via configurational entropy](#)

Low Temp. Phys. **35**, 282 (2009); 10.1063/1.3115806

[Two-level systems/tunnelling modes in glass](#)

AIP Conf. Proc. **489**, 119 (1999); 10.1063/1.1301455



American Association of **Physics Teachers**

Explore the **AAPT Career Center** – access hundreds of physics education and other STEM teaching jobs at two-year and four-year colleges and universities.

<http://jobs.aapt.org>



Fundamentals of PV efficiency interpreted by a two-level model

Muhammad A. Alam^{a)} and M. Ryann Khan

School of Electrical and Computer Engineering, Purdue University, West Lafayette, Indiana 47907, USA

(Received 15 September 2012; accepted 15 June 2013)

We consider the physics of photovoltaic (PV) energy conversion in a two-level, atomic PV and explain the conditions for which the Carnot efficiency is reached and how it can be exceeded. The loss mechanisms—thermalization, angle entropy, and below-bandgap transmission—explain the gap between Carnot efficiency and the Shockley-Queisser limit. Techniques developed to reduce these losses (e.g., solar concentrators, tandem cells, etc.) are reinterpreted using a simple two-level model. Remarkably, this simple model captures the essence of PV operation and reproduces the key results and important insights that have been previously obtained using more complicated derivations. © 2013 American Association of Physics Teachers. [http://dx.doi.org/10.1119/1.4812594]

I. INTRODUCTION

Renewable energy is a topic of broad, current interest. Photovoltaic devices—those that convert radiant energy from the sun into electrical energy—offer a promising source for renewable energy. Because a solar cell is essentially a p-n junction diode illuminated by sunlight, its performance can be understood in terms of a classical diode equation coupled with a current source to account for photogeneration.¹ The key parameters that dictate the efficiency of energy conversion, such as short-circuit current, open-circuit voltage, and fill factor, are easily related to basic diode parameters (doping densities, base and emitter thicknesses, bulk and interface recombinations, etc.^{2,3}), and this detailed understanding of device operation has led to impressive gains in PV efficiency since the 1950s. Coupled with sophisticated process engineering, classical solar cells are beginning to approach the fundamental limits of energy conversion.⁴⁻⁶ Future progress will depend on understanding the origin of the remaining gap between the fundamental and practical limits of PV efficiency.

In this paper, we explain the fundamental limits of energy conversion when a solar cell is viewed as a “photon engine” operating between two reservoirs, the sun and the environment. We discuss the physics of a photovoltaic operation of a collection of two-level atoms. We find that the model anticipates—transparently and intuitively—the fundamental issues of efficiency of a solar cell (many of these results have been derived from far more complicated arguments⁷⁻⁹). The functional relationships derived for the two-level model correctly anticipates the corresponding results for two- and three-dimensional bulk solar cells, except for the numerical coefficients that depend on system dimensionality.

II. PHYSICS OF IDEALIZED 2-LEVEL SYSTEMS

A. 2-level system

Consider a set of two-level “atoms” immersed in an isotropic, three-dimensional field of photons (i.e., the atoms are illuminated from all directions). An analogous problem arises when discussing the physics of photosynthesis in pigment molecules of marine diatoms immersed in a fluid, illuminated by multiply reflected, diffuse (isotropic) light.¹⁰ We will consider discrete levels, although as long as the widths of the bands are much narrower than the energy of the photons, the same conclusions hold. Our goal in this

section is to show that if we could connect these atoms with weak probes to extract the photo-generated electrons, we might be able to achieve or even exceed the Carnot efficiency—the ultimate limit of energy conversion in any thermodynamic engine.

B. Two-level system illuminated by a monochromatic sun

Typically, if the atoms remain in equilibrium with their surrounding of phonons and photons, the relative populations of atoms in the ground state E_2 versus those in the excited states E_1 are governed by the Fermi-Dirac (FD) distribution

$$f_i = \frac{1}{e^{(E_i - \mu_i)/k_B T_D} + 1}, \quad (1)$$

where T_D is the absolute temperature of the 2-level system, k_B is the Boltzmann constant, and μ_i is the electro-chemical potential (or quasi-Fermi levels) associated with the energy level i (1 or 2). Note that $(\mu_1 - \mu_2)_D$ is not necessarily zero. Here, the subscript D represents the “device” (i.e., the 2-level system).

Because the FD distribution is interpreted as the probability of occupation of a state in a bulk semiconductor, one may wonder about the meaning of a FD distribution of a two-level system, where the atoms can either be in the excited state or in the ground state. Here, the probability of occupation reflects the property of the ensemble—the *fraction* of atoms in the up (or down) states are characterized by the FD distribution of those states, appropriately normalized so that the sum of the atoms in the two levels gives the total number of atoms N .

The external isotropic, monochromatic illumination of these atoms (see Fig. 1) changes the relative population by rebalancing the absorption and emission rates. To obtain the fundamental limits, we focus exclusively on radiative recombination and exclude all other non-radiative processes. The absorption or “up” transition is given by

$$U(E_2 \rightarrow E_1) = A f_2 (1 - f_1) n_{ph}, \quad (2)$$

while the emission or “down” transition is given by

$$D(E_1 \rightarrow E_2) = A f_1 (1 - f_2) (n_{ph} + 1). \quad (3)$$

Here, A is a constant, the extra 1 on the right-hand-side of the down transition describes the spontaneous emission (see

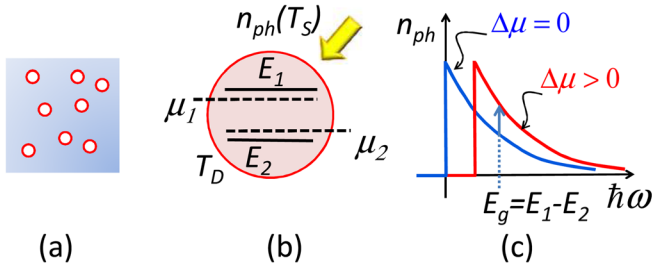


Fig. 1. (a) A collection of 2-level atoms; (b) a 2-level energy system illuminated by photons; (c) the Bose-Einstein distribution.

Feynman, Vol. 3, Chap. 4 for more detailed discussion¹¹), and n_{ph} is the Bose-Einstein (BE) distribution for isotropic photons given by

$$n_{ph}(T_S) = \frac{1}{e^{[(E_1 - E_2) - (\mu_1 - \mu_2)_S]/k_B T_S} - 1} \quad (4)$$

[see Fig. 1(c)]. Here, the subscript S is a reminder that we are talking about photons coming from a “monochromatic sun.” The form of Eq. (4) may be unfamiliar but easily derived. Assume the sun to be an isolated box of atoms and photons in equilibrium at absolute temperature T_S ; equate Eqs. (2) and (3) using Eq. (1) as necessary, and solve for $n_{ph}(T_S)$. Although the sun is powered by internal nuclear reactions, measurement of the solar spectrum shows that $(\mu_1 - \mu_2)_S \equiv \Delta\mu_S \approx 0$.^{1,12} We will use this assumption for the following discussion.

Under an “open-circuit” condition—when electrons are not being extracted from the system—for the two-level system kept at temperature T_D [governed by Eq. (1)] illuminated by photons from a source at temperature T_S [governed by Eq. (4)], the absorption (U) must be balanced by emission (D) so that

$$f_1(1 - f_2)(n_{ph} + 1) = f_2(1 - f_1)n_{ph}. \quad (5)$$

Inserting Eqs. (1) and (4) into Eq. (5) we find that

$$\frac{E_2 - \mu_2}{T_D} + \frac{E_1 - E_2}{T_S} = \frac{E_1 - \mu_1}{T_D}, \quad (6)$$

or equivalently

$$qV_{OC} \equiv (\mu_1 - \mu_2)_D = (E_1 - E_2) \left[1 - \frac{T_D}{T_S} \right]. \quad (7)$$

Here, V_{OC} is the open circuit voltage of the system and q is the electron charge. Notice the appearance of the Carnot factor involving the ratio of the “device” temperature and the temperature of the sun.

Now if we could attach a pair of probes, one exchanging electrons exclusively with E_1 , the other with E_2 (see Fig. 2), to each of the atoms, and if the photon flux R from the sun is small, then the energy input to the ensemble of atoms is $(E_1 - E_2) \times R \times N$, while the maximum energy output is $\sim V_{OC} \times qR \times N = (\mu_1 - \mu_2)_D \times R \times N$, so that the efficiency η is given by (see notes in Ref. 13 for details)

$$\eta = \frac{(\mu_1 - \mu_2)_D R \times N}{(E_1 - E_2) R \times N} = \left[1 - \frac{T_D}{T_S} \right]. \quad (8)$$

We assumed that there is no additional loss introduced by the probes used for carrier extraction.

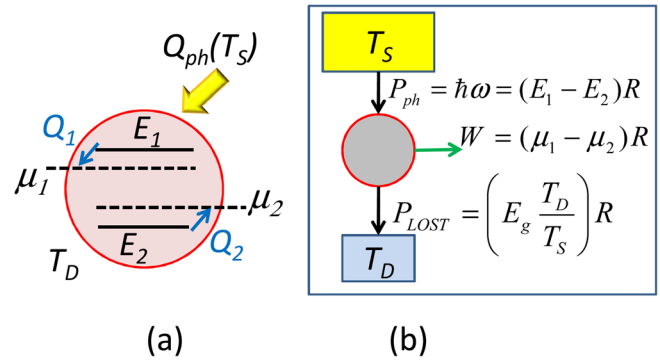


Fig. 2. (a) The energy band for the 2-level system; (b) the energy flux balance of a “photon engine.”

The input and output powers used to derive the efficiency of the 2-level PV system [Eq. (8)] can be represented as a Carnot photon engine. The schematic in Fig. 2(b) makes the analogy between a solar cell and photon engine explicit, and details of entropy considerations are discussed in Appendix B.

In this limit, therefore, a photon engine is just another form of heat engine connected between two reservoirs of temperature T_S and T_D , described by the Carnot formula. Assuming that the atoms are at room temperature ($T_D = 300$ K) and the sun is a blackbody with $T_S = 6000$ K, the efficiency is

$$\eta = \left[1 - \frac{300}{6000} \right] = 0.95. \quad (9)$$

The Carnot’s engine is assumed to work between two reservoirs that are in equilibrium. Interestingly, the efficiency of the system may exceed the Carnot limit if the reservoirs are no longer in equilibrium (this point is discussed in Appendix C).

The conventional PV conversion efficiency limit is 33%, the so-called Shockley-Queisser limit.¹⁴ We will discuss the details of the factors contributing to the losses in practical cells in Sec. III.

C. Two-level atoms with multiple gaps

Let us return to our original discussion of two-level atoms illuminated by isotropic sunlight. In Sec. II A, all the atoms have identical energy gaps and can absorb only at a single energy, and the system achieves the Carnot efficiency. If we generalize the problem so that the ensemble includes N_1 atoms with $E_{G,1} \equiv (E_1^{(1)} - E_2^{(1)})$, N_2 atoms with

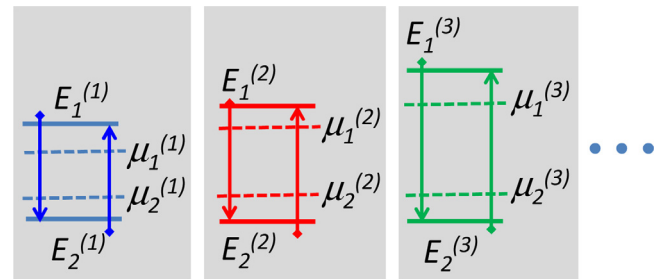


Fig. 3. An ensemble of non-interacting 2-level systems having different energy gaps.

$E_{G,2} \equiv (E_1^{(2)} - E_2^{(2)})$, etc., (see Fig. 3) can the ensemble as a whole still achieve the Carnot efficiency?

The total power input to the system is $P_{in} = \sum_{i=1}^M (E_1^{(i)} - E_2^{(i)}) N_i R$, while the total power-output $P_{out} = \sum_{i=1}^M (\mu_1^{(i)} - \mu_2^{(i)}) N_i R$. As mentioned earlier, R is the photon flux from the sun. The principle of detailed balance requires that each group of atoms is in equilibrium with the corresponding set of incident photons, i.e., $(\mu_1^{(i)} - \mu_2^{(i)}) = \eta_i (E_1^{(i)} - E_2^{(i)})$. Of course, each 2-level system operates at the Carnot efficiency ($\eta_i = \eta_1$). Thus, taken together we have

$$\begin{aligned} \eta_S &= \frac{N_1(\mu_1^{(1)} - \mu_2^{(1)}) + N_2(\mu_1^{(2)} - \mu_2^{(2)}) + \dots}{N_1(E_1^{(1)} - E_2^{(1)}) + N_2(E_1^{(2)} - E_2^{(2)}) + \dots} \\ &= \frac{\eta_1 N_1(E_1^{(1)} - E_2^{(1)}) + \eta_1 N_2(E_1^{(2)} - E_2^{(2)}) + \dots}{N_1(E_1^{(1)} - E_2^{(1)}) + N_2(E_1^{(2)} - E_2^{(2)}) + \dots} \\ &= \eta_1. \end{aligned} \quad (10)$$

The ensemble of atoms absorbing at different frequencies can still achieve the Carnot efficiency, provided the atoms are isolated and energy is independently collected by weakly coupled probes attached to these “atoms.” In the PV literature, solar cells based on such a “spectral splitting technique” have been discussed in the context of very high efficiency cells.¹⁵

III. PHYSICS OF SOMEWHAT REAL PVS: ENSEMBLE OF 2-LEVEL SYSTEMS

Practical limits of solar cells are well known to be far lower than the Carnot limit. Where does the energy go? This dramatic difference of the efficiency between the two-level atomic PV [Eq. (8)] and that of the practical 3D solar cells lies in three factors: the sun is far away and occupies (as a disk) a small fraction of the sky, the dimensionality of the solar cell, and the specific definition of Shockley-Queisser (S-Q) efficiency that includes the below bandgap (the gap between the highest occupied and the lowest unoccupied electronic energy states) light as a loss. We will discuss the three sources of energy losses (see Ref. 16, Chap. 7)—thermalization loss, irreversible generation of entropy due to angle mismatch, and the below bandgap (or transmission) loss—all in the context of the two-level system so that we can understand the gap between real and Carnot-efficient solar cells. For example, a cell operating at the optimum bandgap ($E_g \sim 1.35\text{eV}$) has a thermalization loss of $\sim 30\%$, an angle mismatch loss of $\sim 9\%$, and a below bandgap loss of $\sim 25\%$ of the input solar spectrum.¹⁷

A. Thermalization loss

Let us return to the discussion in Sec. II C where we considered an ensemble of independent atoms illuminated by isotropic sunlight. However, now we assume that the atoms are coupled—as in a solid—so that electrons can transfer from one atom to the next (see Fig. 4). The transfer of electrons from atoms with a larger gap to atoms with a smaller gap is accompanied by the emission of phonons to the environment. We will assume that all the atoms can absorb photons, but photon emission is only possible for atoms with the

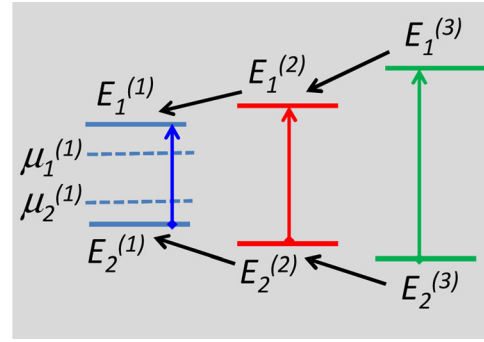


Fig. 4. An ensemble of interacting 2-level systems having different energy gaps.

smallest energy gap ($E_1^{(1)} - E_2^{(1)}$), and energy is only extracted at the smallest gap. In this case, we have

$$\begin{aligned} \eta_S &= \frac{(N_1 + N_2 + N_3 + \dots)(\mu_1^{(1)} - \mu_2^{(1)})}{N_1(E_1^{(1)} - E_2^{(1)}) + N_2(E_1^{(2)} - E_2^{(2)}) + \dots} \\ &= \eta_1 \frac{(N_1 + N_2 + N_3 + \dots)(E_1^{(1)} - E_2^{(1)})}{N_1(E_1^{(1)} - E_2^{(1)}) + N_2(E_1^{(2)} - E_2^{(2)}) + \dots} < \eta_1. \end{aligned} \quad (11)$$

The loss of efficiency is expected because the energy absorbed in atoms with a larger bandgap has been lost to thermalization (phonon emission). Moreover, one can show—by repeating the steps in Appendix B—that the process generates entropy and the system is no longer reversible. In PV parlance, this is called the thermalization loss; it arises from coupling among atoms. An excitonic PV comprising of two coupled 2-level systems provides a particularly elegant example of the importance of thermalization loss, as discussed further in Appendix A.

1. Reducing thermalization loss

Thermalization loss involves energy exchanged to the environment as electrons hop from one atom to the next. Several schemes have been suggested to reduce this loss.

One approach is based on the idea of multiple exciton generation (MEG).^{18,19} In this scheme, the excess energy released as an electron jumps down from one atomic energy level to the next is not lost to phonons but transferred to the acceptor atom itself, so as to thermally generate a new electron-hole pair. Thus, a fraction of the energy lost due to thermalization is revived for energy conversion. Another method to decrease the thermalization loss involves extraction of carriers in excited states before they thermalize. An important consideration for the design of these “hot carrier PVs” is that the thermalization time ($\sim 10\text{--}100\text{ps}$, see Ref. 20) and the carrier transport time to the contacts have to be comparable. This constraint puts an upper limit on the thickness of the solar cells and leads to a trade-off between absorption efficiency and the efficiency of hot-carrier collection. The trade-off could be relaxed by increasing the thermalization time by phononic confinement.²⁰

Another approach to reduce thermalization loss is based on a hybrid photovoltaic/thermal (PV/T) system.²¹ In this scheme circulating fluid collects the waste heat generated by the PV module and uses the heated fluid to run an engine.

[This approach should be distinguished from thermal PV (TPV).²²] Such integrated systems return the efficiency towards the Carnot limit for systems containing multiple atoms with different bandgaps.

B. Angular anisotropy

In the above calculation, multiply scattered, diffused (i.e., isotropic) sunlight was used to illuminate the PV cell. Remarkably, a solar cell illuminated *directly* by the sun has a lower efficiency, as we now explain.

The sun is approximately 150×10^6 kilometers away; therefore, it appears as a small disk in the sky. Hence, the solid angle subtended by the sun is only $\theta_S = 6 \times 10^{-5}$ steradians as seen from the PV cell on the earth [see Fig. 5(a)]. The angle is so small that the rays of sunlight can be considered parallel (and hence the shadow behind an object). On the other hand, when the photons absorbed by the atoms are re-emitted, they are radiated in all directions (radiation angle $\theta_D \sim 4\pi$ steradians). Therefore, Eq. (5) must be rewritten as

$$\theta_D f_1 (1 - f_2) (n_{ph} + 1) = \theta_S f_2 (1 - f_1) n_{ph}, \quad (12)$$

or

$$-\ln\left(\frac{\theta_D}{\theta_S}\right) + \left(\frac{E_2 - \mu_2}{k_B T_D}\right) + \left(\frac{E_1 - E_2}{k_B T_S}\right) = \left(\frac{E_1 - \mu_1}{k_B T_D}\right),$$

which leads to

$$\eta = \frac{\mu_1 - \mu_2}{E_1 - E_2} = \left(1 - \frac{T_D}{T_S}\right) - \frac{k_B T_D}{E_1 - E_2} \ln\left(\frac{\theta_D}{\theta_S}\right). \quad (13)$$

This is a remarkable formula. It says that the efficiency of a photon engine working with direct sunlight is always less than that of an engine operating in isotropic light. To estimate the difference, recall that we have assumed $T_S = 6000$ K and $T_D = 300$ K so that

$$qV_{OC} = \left(1 - \frac{T_D}{T_S}\right) E_g - k_B T_D \ln\left(\frac{\theta_D}{\theta_S}\right) = 0.95 \times E_g - 0.31 \text{ eV}, \quad (14)$$

where $E_g = E_1 - E_2$ (in eV). In other words, for a typical solar cell with a bandgap between 1 and 1.5 eV, almost 30% of the open circuit voltage is lost due to the mismatch between θ_S and θ_D . This corresponds to $\sim 9\%$ loss in energy

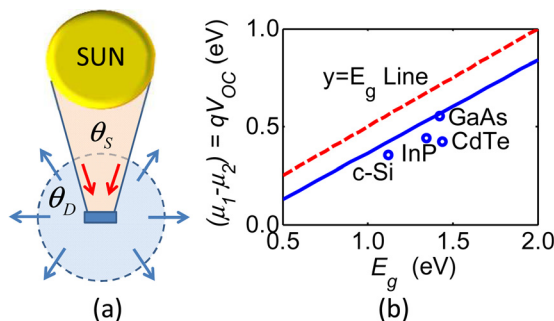


Fig. 5. (a) Angle mismatch between the sun and the solar cell; (b) the open-circuit voltage limit of a PV as a function of bandgap. The blue solid line represents the relationship given by Eq. (15). The experimental results (circles) are taken from Ref. 4.

in practical cells operating at the optimum bandgap of 1.35 eV. For 3D solar cells, the constants in the above equation are slightly different.^{17,23} The loss due to angular anisotropy is partially compensated by the contribution from 3D photonic density of states. Thus the open circuit voltage (3D solar cells) can be approximately represented as

$$qV_{OC} = 0.95 \times E_g - 0.22 \text{ eV}. \quad (15)$$

Remarkably, the best solar cells produced to date all follow Eq. (15), as shown in Fig. 5(b).

I. Isotropic vs. direct sunlight

What is the difference between isotropic vs. direct sunlight that can change the PV efficiency so radically? An atom has certain directivity in the radiation pattern in vacuum.²⁴ In the derivation above, however, we have assumed that the photons arrive and are absorbed in a narrow (solid) angle θ_S , while they reradiate in a broader angle of 4π . This can only happen if the phases of the atoms excited to level 1 are subsequently randomized by the collision among the atoms so that the atoms eventually re-emit with random angles. The entropy gain of a system is $k_B T_D \ln(N_{\text{final}}/N_{\text{initial}})$. Here, the number of radiating angular states is given by $N_{\text{final}} \sim 4\pi$ and the number of angular states occupied by the incoming sunlight is given by $N_{\text{initial}} \sim \theta_S$. We see that the extra loss term can be viewed as an irreversible entropy gain due to angular mismatch between incident and reradiated photons. A complex derivation of this entropy loss exists,¹⁷ but the use of two-level PV makes the physical interpretation intuitive and transparent.

What does it mean to “lose energy” due to angle anisotropy? Let us say that a number of photons enter the solar cell at normal incidence; such photons occupy a specific point in k -space [see Fig. 6(a)]. Absorption of these photons excite the atoms. The atoms then go through a momentum scattering process and subsequently, they collectively emit at random angles [shown in k -space in Fig. 6(b)]. Individually, the photons have the same energy on emission as they did on absorption and there should be no loss of energy. However, we should recognize that it takes energy to create collimated photons (similar to incident sunlight) from random photons emitted by the cell. When the collimated photons are scattered, there is an increase in entropy indicating that some

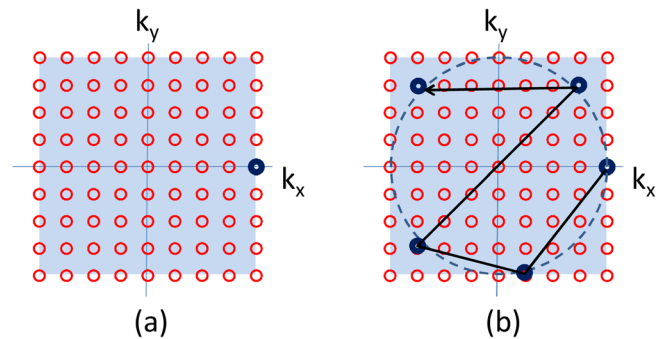


Fig. 6. (a) A single state occupied by a photon (approximately) normally incident from the sun; (b) momentum scattering of the photon inside the solar cell. Note that the photon incidence and re-emission problem is intrinsically three-dimensional, as the atoms can absorb and radiate in 3D patterns; the 2D scheme shown above is used to illustrate the concept of angle entropy.

part of the energy cannot be converted to work. This energy has been irreversibly lost in the process of momentum scattering or angle randomization.

2. Recovery of entropy loss

The efficiency of the solar cell will improve if we can reduce the entropy loss due to angle mismatch. We can either make the absorption angle larger or the emission angle narrower, and both approaches are in practical use today.

a. Mirrors. Solar cells often use mirrors in the back surface, which reflect light and reduces the emission angle from 4π to 2π . Inserting this new angle in Eq. (13), we find that the open circuit voltage increases by $(k_B T_D/q) \times \ln(2)$, or 17 mV at room temperature. This leads to a slight improvement in efficiency.

b. Solar concentrator. If the atoms are placed in a small sphere at the focus of a concentric hemisphere, the atoms will be illuminated from all sides with $(2\pi/\theta_S) \sim 10^5$ suns [see Fig. 7(a)]. The incident angle is now 2π , matching exactly the angle of the radiated photons. In this case, the angular anisotropy term disappears and V_{OC} once again reaches the values corresponding to the Carnot limit. Therefore, the essence of the concentrator solar cells lies in countering the angle entropy generated in a typical solar cell illuminated by direct sunlight.

c. Narrow emission angle. It might be possible to create a set of optical structures so that illumination and emission are possible only with a narrow solid angle [see Fig. 7(b)], as has been suggested in Ref. 25. Depending on the narrowness of the angle, the efficiency should approach the Carnot efficiency for a collection of two-level atoms.

C. Below-bandgap loss

Traditionally, the Shockly-Queisser efficiency of a solar cell is defined by the ratio of energy converted to electricity to total incident energy from the sun. If a photon with energy below (or above) the bandgap passes right through the atoms, never interacting with the atoms themselves, the solar cells will still be held responsible for not being able to convert it to electrical energy. This below-bandgap loss is really not a loss at all, because the photons still carry the memory of the sun and have the ability to do work. The definition presumes that the transmitted energy will be irretrievably lost, and

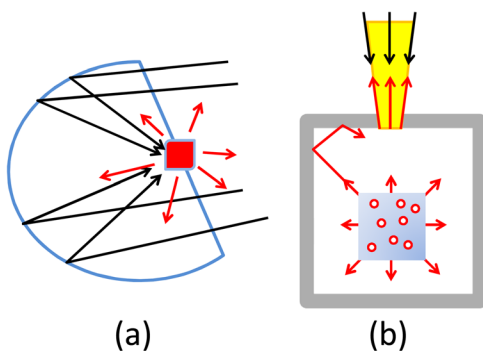


Fig. 7. (a) Angle broadening of incident photons using a solar concentrator; (b) a scheme limiting the emission angle of the PV system.

therefore, should be rightfully chalked up as a loss mechanism.

a. Recovery of below-bandgap loss. Consider, for example, that a quasi-transparent PV has been integrated with the structure of a greenhouse. The below-bandgap photons that escape through solar cells [e.g., large-bandgap organic photovoltaics (OPVs)^{22,26}] can still be used to drive the photosynthesis of the plants placed behind such quasi-transparent PV modules. For smaller bandgap PVs, such as c-Si, the below-bandgap radiation can be used by smaller bandgap materials, such as PVs based on carbon nanotubes.²⁷ Finally, if the PV/T absorber is opaque to below bandgap transmission, a fraction of the below-bandgap energy can also be retrieved. All of these schemes involve interesting examples of a “tandem cell” for high-efficiency energy conversion.

The most interesting scheme to utilize the below-bandgap loss involves thermal PVs (TPVs).²² Here, the first layer absorbs sunlight directly to heat a fluid and re-emits at a lower energy. The second selective emitter layer transmits photons that are easily absorbed by the PV layer in the bottom, but reflects to the absorber the below and above bandgap photons that have previously been lost to below-bandgap transmission and above-bandgap thermalization. These “return-to-sender” photons keep the top absorber layer hot and allows for better conversion efficiency of the PV layer at the bottom.

IV. SUMMARY

An idealized two-level solar cell working in isotropic light is shown to achieve the thermodynamic Carnot efficiency of $\sim 95\%$. In practice, however, three loss mechanisms reduce the efficiency of PV system far below the Carnot limit. The thermalization loss involves asymmetry in energy of the absorption and emission—photons are absorbed in broadband but emitted only in narrowband with the rest of the energy lost to phonons. Hybrid PV/T or MEG systems that recycle the waste heat improve efficiency. The second source of loss involves angle mismatch between direct illumination and emission at random angles, the so-called angle entropy loss. This loss can be reduced either by reducing the emission angle using mirrors or waveguides, or increasing the incident angle using solar concentrators. Finally, the “accounting” or below-bandgap loss can be improved using tandem cells or the TPV approach. Considerations of these loss-mechanisms—within the context of a simple two-level PV system—collectively explain the efficiency degradation from the Carnot limit to the widely known Shockley-Queisser limit.

ACKNOWLEDGMENTS

The authors gratefully acknowledge discussion with Professor J. Gray, Professor M. Lundstrom, and Professor P. Bermel. This material is based upon work supported as part of the Center for Re-Defining Photovoltaic Efficiency Through Molecule Scale Control, an Energy Frontier Research Center funded by the U.S. Department of Energy, Office of Science, Office of Basic Energy Sciences under Award No. DE-SC0001085. The computational resources for this work were provided by the Network of Computational Nanotechnology under NSF Award No. EEC-0228390.

APPENDIX A: THERMALIZATION LOSS IN EXCITONIC PVs

As the simplest example of thermalization loss in coupled two-level atoms, consider an excitonic PV with a donor and an acceptor atom (subsequently referred to as material (1) and material (2), respectively) linked together as a common unit, as shown in Fig. 8. Examples of such donor and acceptor atoms include P3HT and PCBM, respectively.^{26,28} Photons are absorbed in material (1), generating a tightly bound electron-hole pair called an exciton (process 1). The exciton dissociates at the donor/acceptor boundary into a free electron and hole, and the electron transfers to energy level $E_1^{(2)}$ in material (2) (process 2). The free electron at $E_1^{(2)}$ jumps down to an empty state at $E_2^{(1)}$ at the cross gap, producing photons of energy $E_1^{(2)} - E_2^{(1)}$ (process 3). The up and down transitions are given by

$$U(E_1^{(2)} \rightarrow E_1^{(1)}) = Af_2^{(1)}(1 - f_1^{(1)})n_{ph}^U \quad (\text{A1})$$

and

$$D(E_1^{(2)} \rightarrow E_2^{(1)}) = Af_1^{(2)}(1 - f_2^{(1)})(n_{ph}^D + 1). \quad (\text{A2})$$

Here, n_{ph}^U and n_{ph}^D are the BE distributions corresponding to photons having energies $E_1^{(1)} - E_2^{(1)}$ and $E_1^{(2)} - E_2^{(1)}$ respectively. We equate the up and down transitions, Eqs. (A1) and (A2), to obtain

$$(\mu_1^{(2)} - \mu_2^{(1)}) = (E_1^{(2)} - E_2^{(1)}) - \left(\frac{T_D}{T_S}\right)(E_1^{(1)} - E_2^{(1)}). \quad (\text{A3})$$

The corresponding efficiency is

$$\eta_{EX} = \frac{(\mu_1^{(2)} - \mu_2^{(1)})}{(E_1^{(1)} - E_2^{(1)})} = \left(\frac{(E_1^{(2)} - E_2^{(1)})}{(E_1^{(1)} - E_2^{(1)})}\right) - \left(\frac{T_D}{T_S}\right) < \left(1 - \frac{T_D}{T_S}\right). \quad (\text{A4})$$

Note that $E_1^{(2)} - E_2^{(1)} < E_1^{(1)} - E_2^{(1)}$, so from Eq. (A4) we find $\eta_{EX} < \eta_{Carnot}$ and the energy required to dissociate the exciton (step 2) can be viewed as a thermalization loss.

To confirm that Eq. (A4) is consistent with Eq. (11), recall that for a pair of donor and acceptor atoms we have

$$\eta_{EX} = \frac{(N_1 + N_2)(\mu_1^{(2)} - \mu_2^{(1)})}{N_1(E_1^{(1)} - E_2^{(1)}) + N_2(E_1^{(2)} - E_2^{(2)})}. \quad (\text{A5})$$

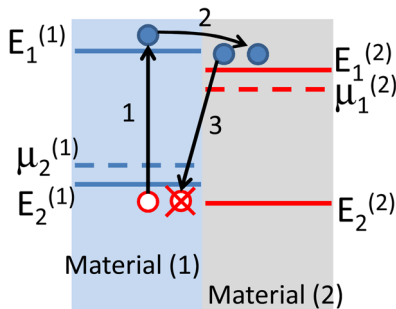


Fig. 8. Schematic diagram showing the operation of an excitonic solar cell.

In this particular case $N_2 = 0$ as there is no absorption in material B, i.e., there is no photon absorption involving $E_1^{(2)} - E_2^{(2)}$. Thus, we find from Eq. (A5) that

$$\eta_{EX} = \frac{(\mu_1^{(2)} - \mu_2^{(1)})}{(E_1^{(1)} - E_2^{(1)})}, \quad (\text{A6})$$

which is precisely the term following the first equal sign in Eq. (A4).

APPENDIX B: ENTROPY BUDGET IN THE PV-SYSTEM

1. Isotropically illuminated 2-level PV

Just to complete the equivalence of the photon engine with a typical reversible thermodynamic engine, let us calculate, based on Fig. 2, the entropy produced in the conversion process by summing up over all the processes involved:

$$\begin{aligned} S &= \sum \frac{Q}{T} = \frac{Q_2}{T_D} + \frac{Q_{ph}}{T_S} - \frac{Q_1}{T_D} \\ &= \frac{E_2 - \mu_2}{T_D} + \frac{E_1 - E_2}{T_S} - \frac{E_1 - \mu_1}{T_D} \\ &= 0, \end{aligned} \quad (\text{B1})$$

where Q_1/T_D and Q_2/T_D are the entropy generated when an electron and a hole exit the contacts respectively, and Q_{ph}/T_S is the entropy produced by photogeneration (see Refs. 26 and 28). This result is not surprising; since the Carnot cycle is reversible there is no net entropy production in the system.

2. Entropy generated by angle anisotropy

Continuing from Sec. III B, a classical derivation of the entropy generated produces the same results:

$$\theta_D f_1(1 - f_2)(n_{ph} + 1) = \theta_S f_2(1 - f_1)n_{ph}, \quad (\text{B2})$$

and therefore

$$\frac{E_2 - \mu_2}{k_B T_D} + \frac{E_1 - E_2}{k_B T_S} = \frac{E_1 - \mu_1}{k_B T_D} + \ln\left(\frac{\theta_D}{\theta_S}\right), \quad (\text{B3})$$

or

$$-S_D^{(2)} + S_{sun} = S_D^{(1)} + S_{angle}, \quad (\text{B4})$$

which gives

$$S_{in} = (S_{out}) + S_{angle}. \quad (\text{B5})$$

Here, $S_{out} = S_D^{(1)} + S_D^{(2)}$; clearly, the angle anisotropy makes the system irreversible.

APPENDIX C: TWO-LEVEL SYSTEM ILLUMINATED BY LIGHT EMITTING DIODES (LEDs)

There is an interesting corollary to the derivation of Eq. (8) presented in Sec. II B. Let us assume that the two-level system is being illuminated in 3D by LEDs rather than by isotropic sunlight (see Fig. 9). Because of the isotropic

incident light, the absorption angle and the emission angle are equal (both are 4π Steradian), so there will be no angle anisotropy loss. Now $(\mu_1 - \mu_2)_{LED} \equiv qV_{LED} > 0$, where the LED is forward biased by V_{LED} . The photons emitted from the LED have nonzero chemical potential $(\mu_1 - \mu_2)_{LED} = \Delta\mu_{LED} > 0$, reflecting the fact that this source does not emit any photon with energy below the bandgap. (The physical meaning of non-zero $\Delta\mu$ for non-equilibrium light sources has been discussed in Ref. 12.)

A recalculation of Eq. (5), using Eqs. (1) and (4) with non-zero $\Delta\mu$, produces

$$\begin{aligned} V_{OC} &\equiv (\mu_1 - \mu_2)_D \\ &= (E_1 - E_2)_D \left[1 - \frac{T_D}{T_{LED}} \right] + (\mu_1 - \mu_2)_{LED} \times \frac{T_D}{T_{LED}}, \end{aligned} \quad (C1)$$

and the efficiency is

$$\eta = \left[1 - \frac{T_D}{T_{LED}} \right] + \frac{T_D}{T_{LED}} \frac{(\mu_1 - \mu_2)_{LED}}{(E_1 - E_2)_D}. \quad (C2)$$

Here $0 < (\mu_1 - \mu_2)_{LED} < (E_1 - E_2)_{LED}$ and $(E_1 - E_2)_{LED} \geq (E_1 - E_2)_D$. The second inequality follows from the requirement that the LED must emit photons at energies that the atoms can absorb. Moreover, one assumes that the emission from the device does not affect the Fermi-level from the source LED. Under these conditions we find $1 > \eta > (1 - T_D/T_S)$ so that the system exceeds the Carnot efficiency!

This intriguing result can be interpreted as follows. A Carnot engine is assumed to operate between two reservoirs, each defined by a temperature T and chemical potential μ . If the reservoirs are not in thermodynamic equilibrium, the quasi-Fermi levels associated with the reservoir will be split. This is indeed the case for LEDs, when it is forward-biased and to be used as a source/reservoir of photons. The LEDs emit photons only at or above the bandgap. Because a solar cell would not be able to use the low energy photons anyway (due to below-bandgap transmission, see Sec. III C), the efficiency of the solar cell—defined by the electrical output to optical input—improves beyond the Carnot limit.

Of course, when we account for the electrical energy necessary for the LED to work, the overall efficiency returns to the Carnot limit. In all fairness, we also do not account for the nuclear reaction inside the sun in our calculation of energy balance. In that strict sense, even a solar illuminated two-level system may exceed the Carnot limit, although the margin of gain is likely to be infinitesimal.

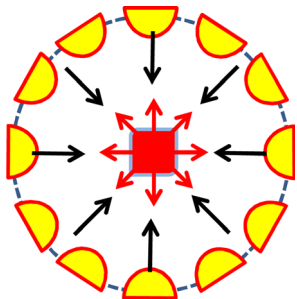


Fig. 9. A PV system isotropically illuminated by LEDs.

Finally, one could say that the photons emitted from the LED have a higher effective temperature $T_{LED}^* > T_{LED}$ and write

$$\eta = \left[1 - \frac{T_D}{T_S} \right] + \frac{T_D}{T_S} \frac{(\mu_1 - \mu_2)_{LED}}{(E_1 - E_2)_D} \equiv \left[1 - \frac{T_D}{T_{LED}^*} \right], \quad (C3)$$

suggesting that the Carnot limit is preserved with the redefined temperature. However, Fig. 1(c) shows that this is not quite correct because the Bose-Einstein distribution n_{ph} for different chemical potentials (μ) cannot be made equal by simply modifying the temperatures; that is, $n_{ph}(\mu_1, T_1) \neq n_{ph}(0, T_1^*)$.

^aElectronic mail: alam@purdue.edu

¹R. F. Pierret, *Advanced Semiconductor Fundamentals* (Prentice-Hall, Upper Saddle River, N.J., 2003).

²M. A. Green, *Solar Cells: Operating Principles, Technology, and System Applications* (Prentice-Hall, Englewood Cliffs, NJ, 1982).

³M. A. Green, *Third Generation Photovoltaics* (Springer-Verlag Berlin Heidelberg, New York, 2006).

⁴M. A. Green, K. Emery, Y. Hishikawa, W. Warta, and E. D. Dunlop, "Solar Cell Efficiency Tables (version 39)," *Prog. Photovolt: Res. Appl.* **20**, 12–20 (2012).

⁵Alta Devices: Finding a Solar Solution—Technology Review, <<http://www.technologyreview.com/energy/39649/>>.

⁶Alta Devices, <<https://www.altadevices.com/>>.

⁷C. H. Henry, "Limiting efficiencies of ideal single and multiple energy gap terrestrial solar cells," *J. Appl. Phys.* **51**, 4494–4500 (1980).

⁸A. Luque and S. Hegedus, *Handbook of Photovoltaic Science and Engineering* (Wiley, Hoboken, NJ, 2003).

⁹J. Nelson, *The Physics of Solar Cells* (Imperial College Press, London, 2004).

¹⁰J. Noyes, M. Sumper, and P. Vukusic, "Light manipulation in a marine diatom," *J. Mater. Res.* **23**, 3229–3235 (2011).

¹¹R. P. Feynman, R. B. Leighton, and M. Sands, *The Feynman Lectures on Physics*, Vol. 3 (Addison-Wesley, 1971).

¹²F. Herrmann and P. Würfel, "Light with nonzero chemical potential," *Am. J. Phys.* **73**, 717–721 (2005).

¹³We have used the fact that for a 2-level solar cell illuminated by a very weak photon flux R , the voltage at the maximum power point (V_{opt}) is asymptotically close to the open circuit voltage (V_{OC}). Thus the maximum energy output is $V_{opt} \times qR \times N \sim V_{OC} \times qR \times N = (\mu_1 - \mu_2)_D \times R \times N$.

¹⁴W. Shockley and H. J. Queisser, "Detailed balance limit of efficiency of p-n junction solar cells," *J. Appl. Phys.* **32**, 510–519 (1961).

¹⁵A. Barnett, C. Honsberg, D. Kirkpatrick, S. Kurtz, D. Moore, D. Salzman, R. Schwartz, J. Gray, S. Bowden, K. Goossen, M. Haney, D. Aiken, M. Wanlass, and K. Emery, "50% Efficient Solar Cell Architectures and Designs," 4th World Conference on Photovoltaic Energy Conversion, IEEE, Vol. 2, pp. 2560–2564 (2006).

¹⁶P. Würfel, *Physics of Solar Cells: From Principles to New Concepts* (Wiley, 2007).

¹⁷L. C. Hirst and N. J. Ekins-Daukes, "Fundamental Losses in Solar Cells," *Prog. Photovolt: Res. Appl.* **19**, 286–293 (2011).

¹⁸S. K. Stubbs, S. J. O. Hardman, D. M. Graham, B. F. Spencer, W. R. Flavell, P. Glarvey, O. Masala, N. L. Pickett, and D. J. Binks, "Efficient carrier multiplication in InP nanoparticles," *Phys. Rev. B* **81**, 081303(R) (2010).

¹⁹S. J. Kim, W. J. Kim, Y. Sahoo, A. N. Cartwright, and P. N. Prasad, "Multiple exciton generation and electrical extraction from a PbSe quantum dot photoconductor," *Appl. Phys. Lett.* **92**, 031107 (2008).

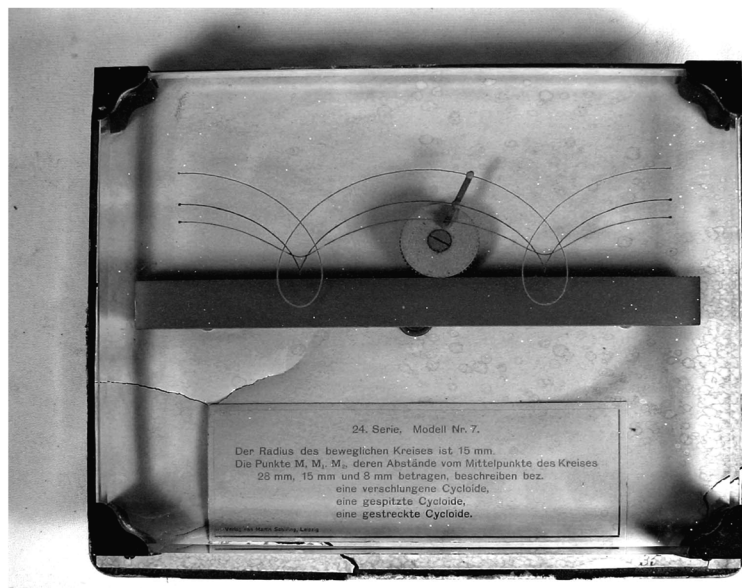
²⁰D. König, K. Casalenuovo, Y. Takeda, G. Conibeer, J. F. Guillemoles, R. Patterson, L. M. Huang, and M. A. Green, "Hot Carrier Solar Cells: Principles, Materials and Design," *Physica E* **42**, 2862–2866 (2010).

²¹T. T. Chow, "A review on photovoltaic/thermal hybrid solar technology," *Appl. Energy* **87**, 365–379 (2010).

²²W. Spirkel and H. Ries, "Solar thermophotovoltaics: An assessment," *J. Appl. Phys.* **57**, 4409–4414 (1985).

- ²³W. H. Press, "Theoretical maximum for energy from direct and diffuse sunlight," *Nature* **264**, 734–735 (1976).
- ²⁴J. P. Dowling, M. O. Scully, and F. DeMartini, "Radiation pattern of a classical dipole in a cavity," *Opt. Commun.* **82**, 415–419 (1991).
- ²⁵Peter Bermel, Michael Ghebrebrhan, Claudia Lau, Xing Sheng, Jurgen Michel, Lionel Kimerling, Marin Soljacic, and Steven G. Johnson, "Correlated randomness for broad-band light-trapping in semiconductor systems," Materials Research Society Fall Meeting in Boston (MA), USA (2011).

- ²⁶B. Ray, P. R. Nair, R. E. Garcia, and M. A. Alam, "Modeling and optimization of polymer based bulk heterojunction (BH) solar cell," Electron Devices Meeting (IEDM), IEEE (2009).
- ²⁷N. M. Gabor, Z. Zhong, K. Bosnick, J. Park, and P. L. McEuen, "Extremely efficient multiple electron-hole pair generation in carbon nanotube photodiodes," *Science* **325**, 1367–1371 (2009).
- ²⁸B. Ray and M. A. Alam, "A compact physical model for morphology induced intrinsic degradation of organic bulk heterojunction solar cell," *Appl. Phys. Lett.* **99**, 033303 (2011).



Cycloid Generator Model

The cycloid is the locus of a point at distance a from the center of a circle of radius r that rolls along a straight line without slipping. For the upper curve, $r < a$, for the middle curve $r = a$, and for the lower curve, $r > a$. Turning a crank on the back of the apparatus moves the gear wheel back and forth along the clogged track, moving the three radial points along the curves painted on the back of the glass. The apparatus is in the Greenslade Collection. (Notes and photograph by Thomas B. Greenslade, Jr., Kenyon College)